Mapping the surface electrostatic potentials of Au(111) by using barrier-height measurements

Takuro Aoki and Takashi Yokoyama*

Department of Nanoscience and Technology, Yokohama City University, 22-2 Seto, Kanazawa-ku, Yokohama 236-0027, Japan

(Received 18 January 2014; revised manuscript received 11 April 2014; published 21 April 2014)

The surface electrostatic potential of Au(111) has been evaluated by using site-specific barrier-height measurements in a scanning tunneling microscope. From the spatial variation of the barrier height, sharp enlargement and reduction of the surface potential are obtained at the upper and lower step edges, respectively, which are characterized as the Smoluchowski effect. We also observe the potential with oscillatory decay away from the step, known as the Friedel potential oscillation. In addition, the periodic potential modulation induced by the surface reconstruction is evaluated quantitatively, which is confirmed by the energy shift of the bulk electronic states.

DOI: 10.1103/PhysRevB.89.155423 PACS number(s): 68.37.Ef, 73.30.+y, 73.20.At

The study of electronic properties on the Au(111) surface have attracted much attention as model systems to study a nearly free two-dimensional (2D) electron gas modified by steps [1,2], spin-orbit coupling [3], and surface reconstructions [4]. The 2D electron gas on the Au(111) surface is originated from a Shockley-type surface state, in which an onset energy and an effective mass have been evaluated [5]. Furthermore, it has been reported that the characteristic $(22 \times \sqrt{3})$ surface reconstruction of Au(111) induces a weak periodic potential acting on the surface-state electrons, leading to the formation of a surface superlattice [4]. The reconstruction is based on a uniaxial compression of the topmost atoms along the $[1\bar{1}0]$ direction, in which 23 surface atoms occupy 22 bulk lattice positions, resulting in alternating fcc and hcp stacking of the surface. The long-range "herringbone" patterns are formed by periodic three-fold rotations of the uniaxial reconstructed domains. This superstructure has been directly characterized by scanning tunneling microscopy (STM) [6,7], and its stability has been confirmed by various theoretical calculations [8–12]. On the superstructure, the reconstruction-induced periodic potentials along the $[1\bar{1}0]$ direction have been reported to be composed of higher and lower maxima on the fcc and hcp domains, respectively, and minima on the bridge sites between the fcc and hcp domains. Bürgi *et al.* [13] numerically derived the potential modulations by using linear response theory from electron density variations, which were measured by integrating dI/dV tunneling spectra. The estimated energies of the potential were $\Delta U_{\mathrm{fcc}} = 37$ meV for the fcc domains and $\Delta U_{\mathrm{hcp}} = 15$ meV for the hcp domains with respect to the minimum energy on the bridge sites. On the other hand, Didiot *et al.* [14] also estimated the energies from opening band gaps in the surface band structure using high-resolution photoemission spectroscopy on Au(111) vicinal surfaces, but the values were $\Delta U_{\mathrm{fcc}} = 140$ meV and $\Delta U_{\mathrm{hcp}} = 48$ meV, significantly larger than Bürgi *et al.*'s values.

In this paper, we report a more direct and precise method to measure the spatial variations of the surface electrostatic potential using low-temperature STM. To determine the surface potential variation ΔU, we measure the local tunneling barrier height $\overline{\phi}$ between the STM tip and the sample surface, which is described as $\overline{\phi} = (\phi_s + \phi_t)/2$ within the Wentzel-Kramers-Brillouin approximation [15], where ϕ_s and ϕ_t are the local work functions of the surface and tip apex, respectively. The surface electrostatic potential U should be directly linked to the local work function ϕ_s of the surface by $U = -\phi_s$ [16], as illustrated in the inset of Fig. 1(a), and thus the local variation should be obtained as $\Delta U = -2\Delta\overline{\phi}$, when ϕ_t is assumed to be constant. Based on this relation, spatial maps of ΔU on the Au(111) surface have been recorded by using barrier-height imaging, showing landscapes of the reconstruction-induced potentials on terraces and Friedel potential oscillations near steps.

The experiments were performed in an ultrahigh-vacuum chamber with a low-temperature scanning tunneling microscope operated at 4.8 K. The Au(111) surface was prepared by Ar^+ sputtering and annealing cycles. Electrochemically etched tungsten tips were used for the STM probe, prepared by Ar^+ sputtering and electron bombardment heating before use. In a simple one-dimensional model, the tunneling current I_t at a fixed low bias is given by

$$I_t \propto \exp\left(-2z\sqrt{\frac{2m}{\hbar^2}\overline{\phi}}\right), \tag{1}$$

where m is the electron mass, $\hbar$ is the reduced Plank constant, and z is the tip-sample distance. The tunneling current I_t as a function of the vertical tip-sample displacement Δz was measured by retracting the tip, and the barrier height $\overline{\phi}$ was derived by fitting to Eq. (1) [17–19]. In addition, the barrier height $\overline{\phi}$ can be also deduced from

$$\overline{\phi} = \frac{\hbar^2}{8m}\left(\frac{d\ln(I_t)}{dz}\right)^2 = \frac{\hbar^2}{8m}\left(\frac{1}{I_t}\frac{dI_t}{dz}\right)^2. \tag{2}$$

To obtain $\overline{\phi}$ as a function of sample bias voltage V_s or tip-sample displacement Δz, we simultaneously measured I_t and dI_t/dz signals by opening the feedback loop with the lock-in detection (622 Hz, 10–40 $\mathrm{pm_{rms}}$ sinusoidal modulation added to z).

Figure 1(a) shows a typical curve of I_t as a function of Δz at a constant bias voltage of $V_s = 50$ mV, which was measured on a terrace of Au(111) at 4.8 K. The mean value of $\overline{\phi}$ was obtained as 5.04 ± 0.09 eV from Eq. (1), which varied by $\approx \pm 0.5$ eV with different tips. The barrier height $\overline{\phi}$ on Au(111) was also obtained from dI/dz spectroscopy using the lock-in

*tyoko@yokohama-cu.ac.jp

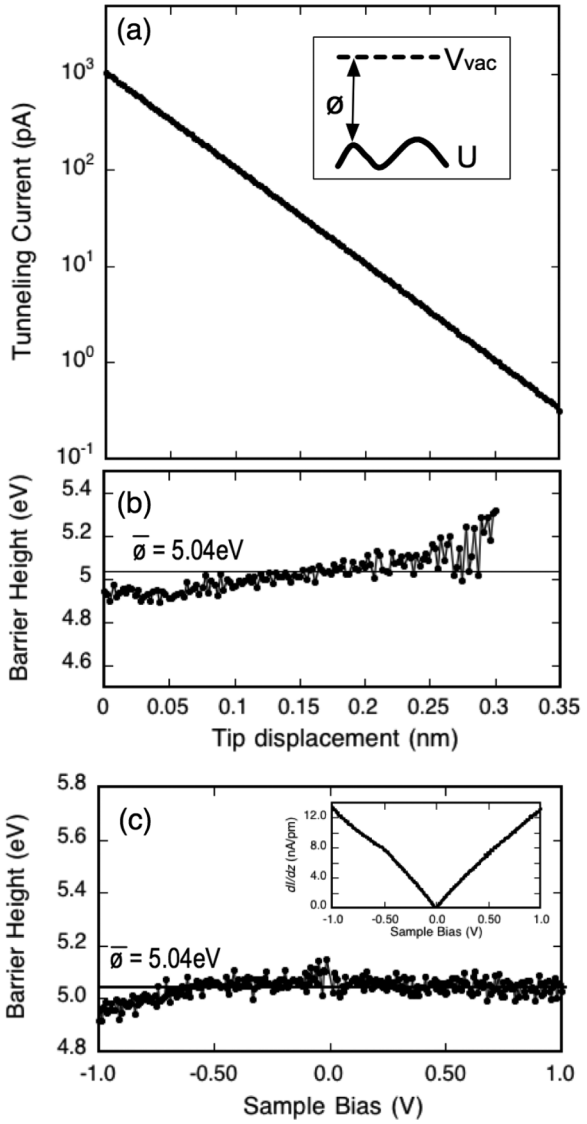

FIG. 1. (a) Tunneling current as a function of the vertical tip-sample displacement, measured on a terrace of the Au(111) surface at 4.8 K. An initial tip position was determined by a tunneling parameter of $V_s = 50$ mV and $I_t = 1.0$ nA, and the current variation at $V_s = 50$ mV was measured during retraction of the tip. The mean value of the barrier height $\overline{\phi} = 5.04 \pm 0.09$ eV was obtained. (b) Barrier height as a function of the vertical tip-sample displacement, which was derived from $I_t(z)$ and $dI_t/dz(z)$ signals measured at the same location as in (a). (c) Barrier height as a function of the sample bias voltage, measured at the same location as in (a). The tip height was initially stabilized by $V_s = 1.0$ V and $I_t = 0.5$ nA, and then $I_t(V)$ and $dI_t/dz(V)$ signals were measured by opening the feedback loop. The inset shows the $dI_t/dz(V)$ spectrum.

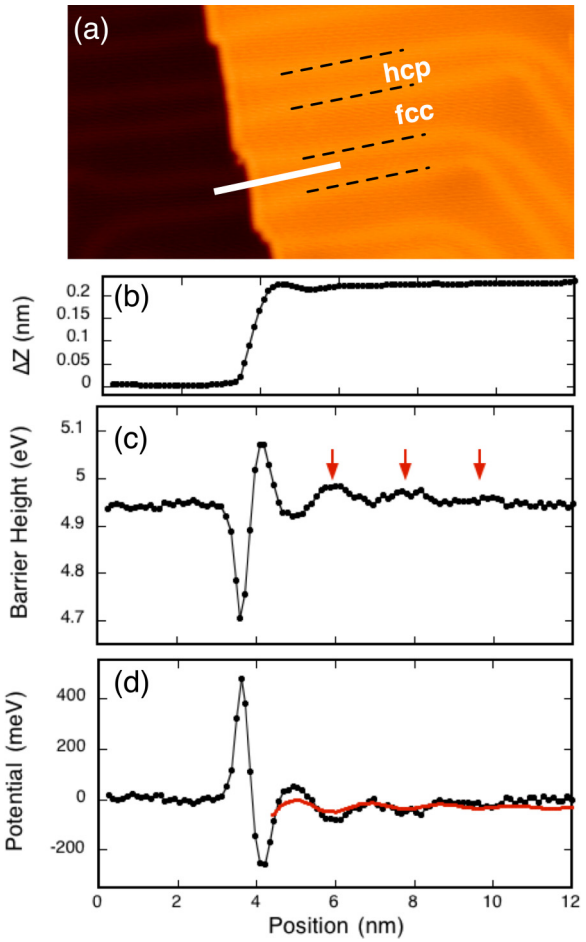

FIG. 2. (Color online) (a) STM image (40×20 nm^2) of Au(111) near a step. (b) Constant-current line scan ($V_s = 1.0$ V, $I_t = 0.5$ nA), measured along the indicated white line in (a), on which the tip was moved while taking $I_t(V)$ and $dI_t/dz(V)$ spectra from $V_s = -100$ mV to 100 mV at a fixed tip-sample separation. (c) Barrier-height variation, derived from the energy-averaged values of $(1/I_t)(dI_t/dz)$ data. (d) Potential variation, derived from (b) using $\Delta U = -2\Delta\overline{\phi}$. A red line indicates the Friedel potential oscillation originated from the formation of electron standing waves, which was calculated using linear response theory with the Lindhard function.

technique with a z modulation at the same location. Figure 1(b) shows the barrier height $\overline{\phi}$ as a function of Δz, evaluated using Eq. (2), which slightly increases with Δz but is almost identical with a mean value of 5.04 eV. We also observed the bias dependence of $\overline{\phi}$ as shown in Fig. 1(c), which was derived from simultaneously obtained $I_t(V)$ and $dI_t/dz(V)$ spectra at a fixed tip-sample separation. In this bias range, $\overline{\phi}$ appears almost constant, whereas $\overline{\phi}$ decreases slightly at higher negative bias. Becker and Berndt [20] reported similar results, in which $\overline{\phi}(V)$ was obtained by constant-current dI/dz spectroscopy. In our measurements, $\overline{\phi}$ should be sufficiently constant in a lower bias range ($|V_s| < 500$ mV), so that the energy-averaged values of $\overline{\phi}$ within ± 100 mV were evaluated from $\overline{\phi}(V)$ spectra to extract the spatial variations of $\Delta U = -2\Delta\phi$.

Figure 2(a) shows a STM image of the Au(111) surface near a step, in which striped reconstruction patterns appear on terraces. A series of the barrier height $\overline{\phi}$ was measured along the indicated line on a hcp domain across a step in Fig. 2(a), which was deduced from $I(V)$ and $dI/dz(V)$ spectroscopy with a fixed tip-sample separation at each point. Figure 2(b) shows a constant-current line scan obtained during the barrier height measurements, in which the height variation taken at $V_s = 1.0$ V is almost unaffected by electron standing waves, so that the tip should trace the actual topography. The obtained variation of $\overline{\phi}$ is shown in Fig. 2(c), revealing a sharp peak

and valley at the upper and lower step edges, respectively. Due to the tip dependency, the mean value of $\overline{\phi} = 4.95$ eV on the terrace is slightly different from that ($\overline{\phi} = 5.04$ eV) in Fig. 1. At the step edge, the local reduction in $\overline{\phi}$ has been known as the Smoluchowski effect [21], which results from a charge redistribution with electron transfer from upper to lower step edges. The resultant dipole formation reduces the work function locally. Similar reduction in the barrier height has been observed on metal surfaces by STM at room temperature [22]. On the other hand, we also observed the local enlargement in $\overline{\phi}$ at the upper step edges, which should be associated with the local electron depletion due to the electron transfer [21]. From the theoretical calculations with the use of the full-potential linearized augmented plane-wave method, such a peak-and-valley shape of the local work function has been expected on Pd surfaces [23].

In addition to the peak-and-valley shape, small periodic variation of $\overline{\phi}$ decaying away from the step edge appears in Fig. 2(c), the periodicity of which was estimated at about 1.8 nm. Since this periodicity is close to the half Fermi wavelength of the surface states on Au(111), the oscillatory decay in $\overline{\phi}$ should be associated with the standing waves of the electron density. In the vicinity of steps, the electron standing waves result from scattering of surface-state electrons, and the resultant redistribution of electron density should lead to the formation of the external potential [24], known as the Friedel potential oscillations [25]. Figure 2(d) shows the spatial variations in ΔU deduced from the relationship as $\Delta U = -2\Delta\phi$. To compare with the Friedel potential oscillations, we calculated oscillatory potential from the electron density distributions of the standing waves using linear response theory with the Lindhard function [26]. As shown by the red line in Fig. 2(d), the calculated potential oscillations are almost in agreement with the experimental variation.

In addition to the potential variation near steps, we investigated the surface-reconstruction-induced potential of Au(111). Figures 3(b) and 3(c) show the obtained spatial variations in $\overline{\phi}$ and ΔU, respectively, along the [1$\bar{1}$0] direction across the striped pattern. The constant-current line scan shown in Fig. 3(a) is close to the physical height of the surface atoms predicted by first-principles calculations using density functional theory [12], so the influence of the inaccurate tip height variations on the barrier height should be neglected [27].

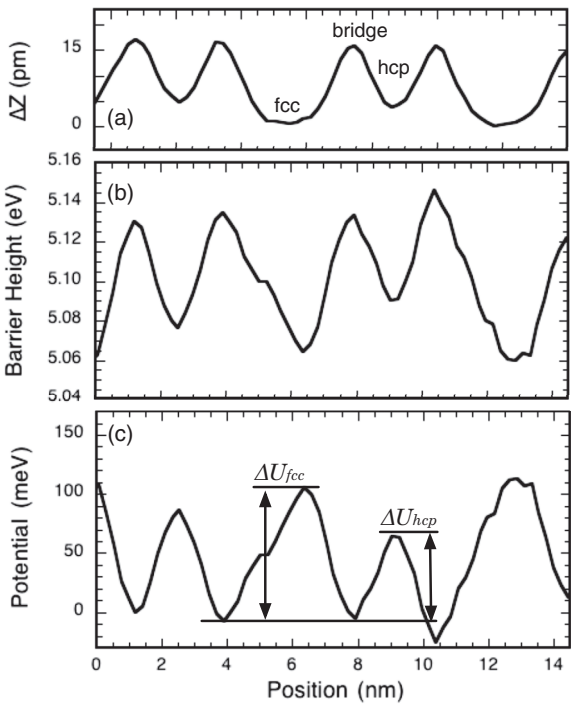

FIG. 3. (a) Constant-current line scan ($V_s = 1.0$ V, $I_t = 0.5$ nA), measured along the [1$\bar{1}$0] direction across fcc, hcp, and bridge regions of the surface reconstruction, on which the tip was moved while taking $I_t(V)$ and $dI_t/dz(V)$ spectra from $V_s = -100$ mV to 100 mV. (b) Barrier-height variation, derived from the energy-averaged values of $(1/I_t)(dI_t/dz)$ data. (c) Potential variation, derived from (b). The averaged potentials were estimated as $\Delta U_{\rm fcc} = 100 \pm 20$ meV for fcc domains and $\Delta U_{\rm hcp} = 65 \pm 10$ meV for hcp domains from more than 10 line scans.

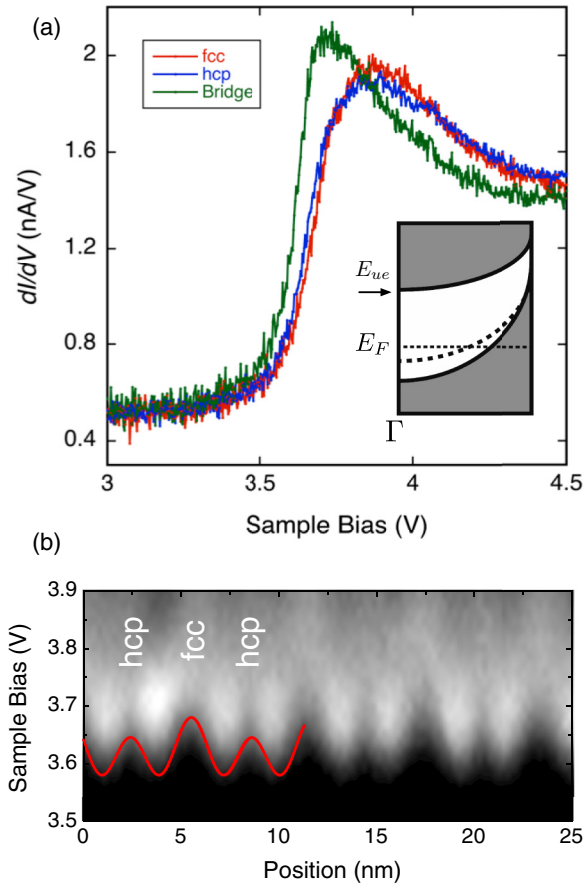

FIG. 4. (Color online) (a) dI_t/dV tunneling spectra obtained at fcc, hcp, and bridge domains at 4.8 K, which were recorded at a constant current of 500 pA by closing the feedback loop with the lock-in detection with a bias modulation (10 mV, 622 Hz). The inset shows a schematic illustration of the electronic surface band structure. E_{ue} denotes the upper edge of the projected band gap. (b) A series of the dI_t/dV spectra obtained across the striped reconstruction pattern. A red line shows the potential variation obtained by the barrier-height measurements, which was vertically shifted to be compared with the dI_t/dV spectra.

The shape of ΔU in Fig. 3(c) resembles the previously reported results [13,14], which are composed of higher and lower maxima on the fcc and hcp domains, respectively, and minima on the bridge sites, as mentioned above. Although Kurokawa *et al.* [28] reported the local reduction in $\overline{\phi}$ (local enlargement in ΔU) at the bridge region at room temperature, we did not reproduce it. The averaged potential energies obtained from more than 10 line scans were evaluated to be $\Delta U_{\mathrm{fcc}} = 100 \pm 20$ meV for fcc domains and $\Delta U_{\mathrm{hcp}} = 65 \pm 10$ meV for hcp domains with respect to the bridge region as indicated in Fig. 3(c), which are close to those ($\Delta U_{\mathrm{fcc}} = 140$ meV, $\Delta U_{\mathrm{hcp}} = 48$ meV) by Didiot *et al.* [14], while significantly larger than those ($\Delta U_{\mathrm{fcc}} = 37$ meV, $\Delta U_{\mathrm{hcp}} = 15$ meV) by Bürgi *et al.* [13].

The surface-reconstruction-induced potential was also investigated from an energy shift in the bulk electronic states. Figure 4(a) shows constant-current dI/dV spectra obtained at fcc, hcp, and bridge regions, in which a steplike increase at $V_s \approx 3.6$ V has been assigned to the upper edge E_{ue} of the projected bulk band gap at Γ [20,29], as illustrated in the inset. It is clearly visible that the onset energies are slightly shifted by measuring locations, which should be associated with the spatial variations of the local work function ϕ_s (external potential). Since the spectral shapes (slopes) were changed by the locations, it is difficult to accurately evaluate the shifts of the onset energies. Roughly estimated values of the onset energy shifts were about 80 mV for fcc domains, and 50 mV for hcp domains with respect to the onset energy at the bridge region, almost in accordance with the potential energies evaluated by the barrier-height measurements [see Fig. 3(c)]. Figure 4(b) shows a direct comparison between the potential energy variation and a series of dI/dV spectra taken along the $[1\bar{1}0]$ direction across the striped pattern. It is clear that the obtained potential is well reproduced by the local energy shifts of the bulk electronic states.

Our obtained potentials ΔU_{fcc} and ΔU_{hcp} are significantly larger than those by Bürgi *et al.* [13]. Nevertheless, the potential difference $\Delta U_{\mathrm{fcc-hcp}}$ between fcc and hcp regions is almost identical within error ($\Delta U_{\mathrm{fcc-hcp}} = 35$ meV for our result and 22 meV for Bürgi *et al.*'s result), although Didiot *et al.*'s result ($\Delta U_{\mathrm{fcc-hcp}} = 92$ meV) [14] is distinct. These values are also in agreement with $\Delta U_{\mathrm{fcc-hcp}} = 25$ meV obtained based on the extended Kronig-Penny potential by Chen *et al.* [4]. Thus, the discrepancy in ΔU_{fcc} and ΔU_{hcp} should arise from the overestimation of the potential at the bridge region by Bürgi *et al.* Based on the linear response theory, they extracted the potential maps using the Fourier and inverse Fourier transformation of the surface electron densities. Due to the complex procedures, the sharp potential dip at the bridge region could not be traced precisely.

In summary, we presented a method to measure spatial variations of surface electrostatic potential using barrier-height imaging. In the vicinity of steps, sharp peak-valley shapes and oscillatory decay were observed in the potential variation and were associated with the Smoluchowski effect and Friedel potential oscillation, respectively. In addition, the periodic potential modulation induced by the surface reconstruction of Au(111) was evaluated quantitatively, which was in agreement with the energy shift of the bulk electronic states. We believe that this method should be applied to probe various surface electrostatic potentials. Recently, the spin-dependent Smoluchowski effect has been observed at a step of a Co nanoisland [30]. In this system, spin-related potential variation might be observable.

We would like to thank Dr. Felix Hanke and Dr. Jonas Björk for several comments about the reconstruction-induced potential. This work was financially supported by grants-in-aid from the Japanese Society for the Promotion of Science.

[1] Y. Hasegawa and Ph. Avouris, Phys. Rev. Lett. **71**, 1071 (1993).
[2] Ph. Avouris and I.-W. Lyo, Science **264**, 942 (1994).
[3] S. LaShell, B. A. McDougall, and E. Jensen, Phys. Rev. Lett. **77**, 3419 (1996).
[4] W. Chen, V. Madhavan, T. Jamneala, and M. F. Crommie, Phys. Rev. Lett. **80**, 1469 (1998).
[5] S. D. Kevan and R. H. Gaylord, Phys. Rev. B **36**, 5809 (1987).
[6] Ch. Wöll, S. Chiang, R. J. Wilson, and P. H. Lippel, Phys. Rev. B. **39**, 7988 (1989).
[7] J. V. Barth, H. Brune, G. Ertl, and R. J. Behm, Phys. Rev. B **42**, 9307 (1990).
[8] N. Takeuchi, C. T. Chan, and K. M. Ho, Phys. Rev. B **43**, 13899 (1991).
[9] S. Narasimhan and D. Vanderbilt, Phys. Rev. Lett. **69**, 1564 (1992).
[10] H. Bulou and C. Goyhenex, Phys. Rev. B **65**, 045407 (2002).
[11] Y. Wang, N. S. Hush, and J. R. Reimers, Phys. Rev. B **75**, 233416 (2007).
[12] F. Hanke and J. Björk, Phys. Rev. B **87**, 235422 (2013).
[13] L. Bürgi, H. Brune, and K. Kern, Phys. Rev. Lett. **89**, 176801 (2002).
[14] C. Didiot, Y. Fagot-Revurat, S. Pons, B. Kierren, C. Chatelain, and D. Malterre, Phys. Rev. B **74**, 081404 (2006).
[15] J. G. Simmons, J. Appl. Phys. **34**, 1793 (1963); **34**, 2581 (1963).
[16] K. Wandelt, Appl. Surf. Sci. **111**, 1 (1997).
[17] G. Binning, H. Rohrer, Ch. Gerber, and E. Weibel, Appl. Phys. Lett. **40**, 178 (1982).
[18] N. D. Lang, Phys. Rev. B **37**, 10395 (1988).
[19] L. Olesen, M. Brandbyge, M. R. Sørensen, K. W. Jacobsen, E. Lægsgaard, I. Stensgaard, and F. Besenbacher, Phys. Rev. Lett. **76**, 1485 (1996).
[20] M. Becker and R. Berndt, Phys. Rev. B **81**, 035426 (2010).
[21] R. Smoluchowski, Phys. Rev. **60**, 661 (1941).
[22] J. F. Jia, K. Inoue, Y. Hasegawa, W. S. Yang, and T. Sakurai, Phys. Rev. B **58**, 1193 (1998).
[23] I. Merrick, J. E. Inglesfield, and G. A. Attard, Phys. Rev. B **71**, 085407 (2005).
[24] M. Ono, Y. Nishigata, T. Nishio, T. Eguchi, and Y. Hasegawa, Phys. Rev. Lett. **96**, 016801 (2006).
[25] J. Friedel, Nuovo Cimento Suppl. **7**, 287 (1958).

[26] The electrostatic potential was obtained from the calculated electron density of the surface states near a step edge, based on Ref. [13]. At the step edge, a hard-wall barrier for the 2D surface-state electrons with $m^* = 0.27m_e$ and $E_0 = -0.51$ eV is assumed, and the electron density was evaluated by the integral of the local density of states of the standing waves.

[27] Since the reconstruction corrugation (within 0.02 nm) is very small, such an influence is expected to be negligible from Fig. 1(b). Nevertheless, the potential variation is also very small, and thus we have experimentally confirmed that the potential variation is almost independent of the line-scan parameters.

[28] S. Kurokawa, Y. Yamashita, A. Sakai, and Y. Hasegawa, Jpn. J. Appl. Phys. **40**, 4277 (2001).

[29] D. P. Woodruff, W. A. Royer, and N. V. Smith, Phys. Rev. B **34**, 764 (1986).

[30] O. P. Polyakov, M. Corbetta, O. V. Stepanyuk, H. Oka, A. M. Saletsky, D. Sander, V. S. Stepanyuk, and J. Kirschner, Phys. Rev. B **86**, 235409 (2012).